

# Surfactant-free CO<sub>2</sub>-based microemulsion-like systems†

 Robert F. Hankel,<sup>‡,a</sup> Paula E. Rojas,<sup>‡,bc</sup> Mary Cano-Sarabia,<sup>bc</sup> Santi Sala,<sup>bc</sup>  
Jaume Veciana,<sup>bc</sup> Andreas Braeuer\*<sup>a</sup> and Nora Ventosa\*<sup>bc</sup>

 Cite this: *Chem. Commun.*, 2014, 50, 8215

 Received 10th March 2014,  
Accepted 30th May 2014

DOI: 10.1039/c4cc01804d

[www.rsc.org/chemcomm](http://www.rsc.org/chemcomm)

**The presence of water-rich and water-lean nanodomains in a transparent, pressurized “water–acetone–CO<sub>2</sub>” mixture was revealed by Raman spectroscopy. This nano-structured liquid can be classified as a surfactant-free microemulsion-like system and has the capacity to dissolve hydrophobic compounds, such as ibuprofen, in the presence of large amounts of water. This finding opens new opportunities in the fields of confined reactions and material templating.**

Microemulsions were introduced in 1943 by Hoar and Schulman,<sup>1</sup> who titrated a milky emulsion with hexanol yielding a transparent one. Since that time microemulsions have attracted increasing attention because of their numerous product applications. Microemulsion-like systems are macroscopically isotropic mixtures of at least one hydrophilic, one hydrophobic and one amphiphile compound. They differ from conventional emulsions in their thermodynamic stability and nanostructure.<sup>2,3</sup> Since microemulsions contain a polar as well as a nonpolar compound, they are capable of solubilizing a wide spectrum of solutes and thus are a versatile reaction medium with applications ranging from nanoparticle templating to preparative organic chemistry. Because of its spatial confinement, the dispersed phase of the microemulsions can be used as nano-reactors with unique interfacial properties. Microemulsions feature a straightforward one-step formation procedure, without elaborate synthetic stages.<sup>4</sup> “Green Chemistry” ambitions motivate attempts to produce

microemulsion with a reduced amount of surfactants or – in the best case – without any surfactant. Even though surfactant-free microemulsions have been known since the late 1970s, only scarce papers deal with this topic.<sup>5–8</sup>

Here we report for the first time – to the best of the authors’ knowledge – a surfactant-free pressurized microemulsion-like system composed of water, acetone and CO<sub>2</sub> showing the capability of solubilizing ibuprofen, a hydro- and CO<sub>2</sub>-phobic compound, which is soluble in CO<sub>2</sub>-expanded acetone. CO<sub>2</sub>-based microemulsions containing surfactants are known,<sup>9–13</sup> but not surfactant-free ones.<sup>5,14</sup>

Unlike water, CO<sub>2</sub> is nonpolar and features weak van der Waals forces, even if compressed. Thus, water and CO<sub>2</sub> represent extremes among the solvents. Therefore, pressurized microemulsions containing water as well as compressed CO<sub>2</sub> have the potential to act as universal solvents for a wide variety of solutes.<sup>10</sup>

The phase behavior of ternary mixtures of water, acetone and CO<sub>2</sub> at high pressure has been the subject of many studies revealing a high pressure fluid–fluid phase equilibrium.<sup>15,16</sup> Therefore, according to a phenomenon called “salting out with a supercritical fluid” which was first described by Elgin and Weinstock in the late 1950s, initially homogeneous mixtures of acetone and water can be split in two fluid phases by pressurization with CO<sub>2</sub>.<sup>17</sup>

We have used Raman spectroscopy to gain an insight at the molecular level of the effect of the addition of compressed CO<sub>2</sub> over a mixture of water and acetone, before the system separates in two liquid phases. Vibrational spectroscopy allows probing the local environment of a molecule.<sup>18</sup> Therefore, Raman spectroscopy provided insights into the state of aggregation of water molecules in the ternary systems at high pressure. The existence of the microemulsion-like system is proven from the Raman spectrum of the OH stretch vibration of the water molecules, which gives insights into the development of the hydrogen bonding on a molecular level. The broad Raman spectrum of the OH stretch vibration of liquid water covers the wavenumber range between 3050 and 3850 cm<sup>-1</sup> and can be deconvoluted into several single peaks, representing different states of hydrogen bonding between the water molecules.<sup>19</sup> While the number and

<sup>a</sup> *Lehrstuhl für Technische Thermodynamik (LTT) and Erlangen Graduate School in Advanced Optical Technologies (SAOT) Friedrich-Alexander Universität Erlangen-Nürnberg, Paul-Gordan-Strasse 6, 91052 Erlangen, Germany. E-mail: Andreas.Braeuer@fau.de; Tel: +49 9131 8525853*

<sup>b</sup> *Department of Molecular Nanoscience and Organic Materials, Institut de Ciència de Materials de Barcelona (ICMAB-CSIC), Campus la Universitat Autònoma Barcelona (UAB), 08193 Bellaterra, Spain. E-mail: ventosa@icmab.es; Tel: +34 935801853*

<sup>c</sup> *CIBER-BBN: Campus Río Ebro - Edificio I+D Bloque 5, 1ª planta C/ Poeta Mariano Esquillor s/n, 50018 Zaragoza, Spain*

† Electronic supplementary information (ESI) available: Materials, ibuprofen solubilization experiments, experimental procedures for Raman spectroscopy acquisition and data treatment. See DOI: 10.1039/c4cc01804d

‡ These authors contributed equally.



the central wavenumber positions of the single peaks are still debated, there is a general consensus in the literature that the low wavenumber Raman signals (here between 3050 and 3450  $\text{cm}^{-1}$ ) can be assigned to the hydrogen bonded water molecules and that the high wavenumber Raman signals (here between 3450 and 3850  $\text{cm}^{-1}$ ) can be assigned to least bonded water molecules. We set the wavenumber position of the temperature-isosbestic point<sup>20</sup> of the Raman OH stretch vibration of pure liquid water at 3450  $\text{cm}^{-1}$ , the border between bonded and least (here called “non-bonded”) Raman signals. Along this communication the Raman signals assignable to the non-hydrogen-bonded and to the hydrogen-bonded water molecules are referred to as  $I_{\text{nb}}$  and  $I_{\text{b}}$ , respectively. Furthermore, we use  $R_{\text{OH}}$  as the ratio  $I_{\text{b}}/I_{\text{nb}}$ . A detailed description of the determination of  $R_{\text{OH}}$  from the acquired raw Raman spectra is given in the ESI.† Temperature,<sup>21</sup> composition<sup>22</sup> or density<sup>23</sup> variations in the systems influence the development of the hydrogen bonding, and are therefore observable in the OH stretch vibration Raman spectrum of water and consequently influence  $R_{\text{OH}}$ .

In order to demonstrate the existence of a microemulsion-like system composed of acetone, water and  $\text{CO}_2$  we carried out two Raman experiments. We diluted an equimolar mixture of acetone and water at 10 MPa and 308 K isobaric and isothermal, once by the addition of acetone and once by the addition of  $\text{CO}_2$ . During the addition of acetone or  $\text{CO}_2$  we kept the pressure constant by increasing the volume of the pressurized system. For both experiments we computed the ratio  $R_{\text{OH}}$  from the OH stretch vibration Raman signal of water to monitor the evolution of the development of the hydrogen bonding between the water molecules. It should be mentioned here that at 10 MPa and 308 K,  $\text{CO}_2$  shows low solubility in water, whereas it is completely miscible with acetone.<sup>24</sup> Fig. 1 shows the two mixing paths in a triangle phase composition diagram when either acetone or  $\text{CO}_2$  are added to the equimolar acetone–water mixture. Furthermore the evolutions of  $R_{\text{OH}}$  are given as a function of the water molar fraction  $x_{\text{H}_2\text{O}}$ . It should be mentioned here that a decrease of the water mole fraction goes in hand with an increase of the volume for all the reported experiments. If acetone is added to dilute the equimolar mixture,  $R_{\text{OH}}$  decreases continuously as a function of the decreasing molar fraction  $x_{\text{H}_2\text{O}}$  within the analyzed range. This indicates a continuous decrease of the number of hydrogen bonded water molecules (proportional to  $I_{\text{b}}$ ) relative to the number of non-bonded water molecules (proportional to  $I_{\text{nb}}$ ). The dilution by the addition of acetone increases the mean distance between the water molecules and therefore weakens the hydrogen bonds. This effect, which is based on the consideration of the mean distance between the water molecules, is referred to as dilution effect.

If  $\text{CO}_2$  is added to dilute the initially equimolar acetone–water mixture,  $R_{\text{OH}}$  first decreases ( $0.50 > x_{\text{H}_2\text{O}} > 0.45$ ) and later increases ( $0.45 > x_{\text{H}_2\text{O}} > 0.41$ ) with decreasing molar fraction of water ( $x_{\text{H}_2\text{O}}$ ). As observed in Fig. 1, the initial  $R_{\text{OH}}$  decrease is not as strong as when adding acetone. Therefore, another effect occurs in the system that counteracts the dilution effect. From  $x_{\text{H}_2\text{O}} = 0.45$ ,  $R_{\text{OH}}$  increases with decreasing  $x_{\text{H}_2\text{O}}$ , indicating that this second effect is now stronger. In the

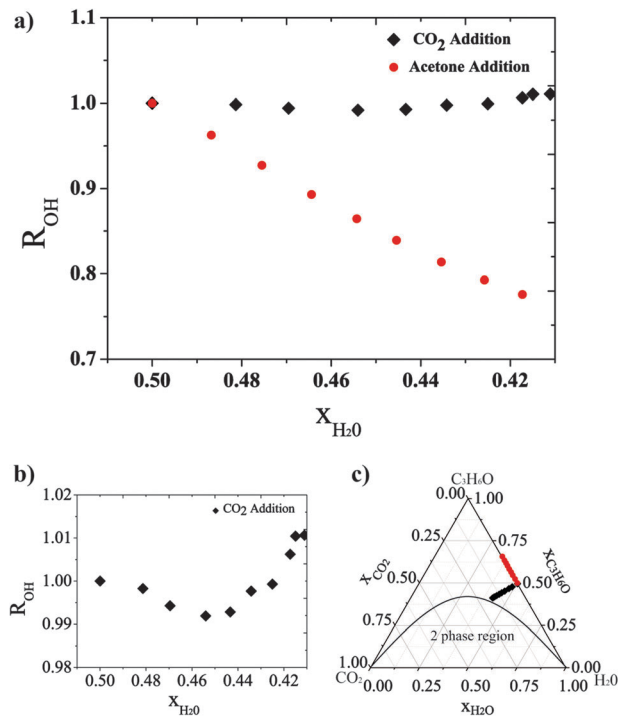


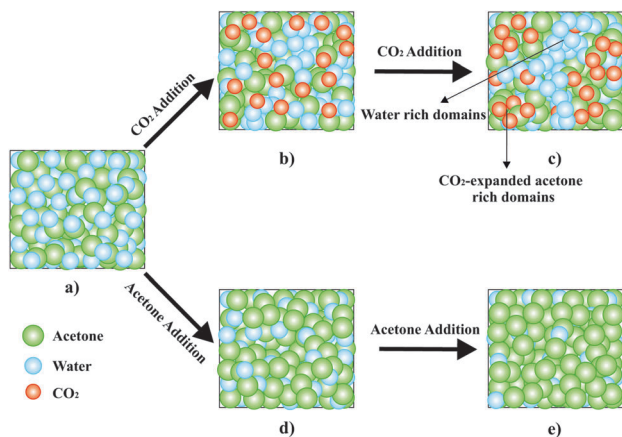
Fig. 1 (a) Evolution of the  $R_{\text{OH}}$  ratio as a function of  $x_{\text{H}_2\text{O}}$  of the mixtures, during the progressive addition of  $\text{CO}_2$  (black diamonds) and acetone (red dots), at 10 MPa and 308 K, over an initial equimolar mixture of acetone and water; (b) a zoom of the  $R_{\text{OH}}$  ratio evolution during the progressive addition of  $\text{CO}_2$ ; (c) the composition evolution of the system upon progressive addition of  $\text{CO}_2$  (black diamonds) and acetone (red dots) represented in a ternary diagram.

further progress of this communication this second effect is called clustering effect. Scheme 1 shows the dilution effect for the addition of acetone and the clustering effect for the addition of  $\text{CO}_2$  to the initially equimolar acetone–water mixture. With respect to the evolution of  $R_{\text{OH}}$  represented as a function of  $x_{\text{H}_2\text{O}}$  in Fig. 1, the addition of  $\text{CO}_2$  first increases the effective distance between the water molecules, which is represented by a decrease of  $R_{\text{OH}}$  for water molar fractions above 0.45. For molar fractions below 0.45 the addition of more  $\text{CO}_2$  has to promote the formation of water clusters, in which the effective distance between the water molecules decreases, while at the same time the mean distance between the water molecules in the system still increases with further dilution. In other words, the system is still homogeneous on a macroscopic scale, but inhomogeneous on a molecular level.

If the water molecules cluster to water-rich regions, as shown in Scheme 1, other water-lean nanoscopic regions should exist with higher acetone and  $\text{CO}_2$  content relative to the bulk. These nanodomains of different compositions are supposed to be organized at the nanoscopic scale forming a macroscopically homogeneous single phase, which shows the physical characteristics of a surfactant-free microemulsion-like system.

In order to further support the existence of  $\text{CO}_2$ -expanded acetone nanodomains in this nanostructured and macroscopically homogeneous microemulsion-like system, we studied the power of the microemulsion to dissolve a non-water and





**Scheme 1** Difference of adding acetone or CO<sub>2</sub> to the initial mixture. (a) Mixture of water and acetone; (b) addition of CO<sub>2</sub> first dilutes the system and increases the mean distance between the water molecules; (c) formation of water-rich and water-lean regions is initiated by adding more CO<sub>2</sub>. (d) and (e) Addition of acetone dilutes the system and increases the mean and the effective distance between the water molecules.

non-CO<sub>2</sub> soluble compound. Then we compared the results with the solvation capacity of a CO<sub>2</sub>-free equimolar acetone-water mixture. We chose ibuprofen, which is a widely used anti-inflammatory substance with a poor solubility in water and CO<sub>2</sub> ( $0.18 \times 10^{-5} \text{ mol mol}^{-1}$  ref. 25 and  $0.13 \times 10^{-2} \text{ mol mol}^{-1}$  ref. 26 respectively), but which has a high solubility in CO<sub>2</sub>-expanded acetone at 10 MPa and 308 K.<sup>27</sup>

As shown in Fig. 2, the addition of CO<sub>2</sub> over an equimolar water-acetone mixture saturated with ibuprofen, where a solid phase and a liquid phase coexist, at 10 MPa and 308 K causes unexpectedly the solubilization of the precipitated CO<sub>2</sub>-phobic drug. This unforeseen behavior is clearly explained if the addition of CO<sub>2</sub> causes a structuring at the nanoscale in water rich regions and in water lean, CO<sub>2</sub>-expanded acetone domains, where the ibuprofen is dissolved. Therefore the ibuprofen experiments as

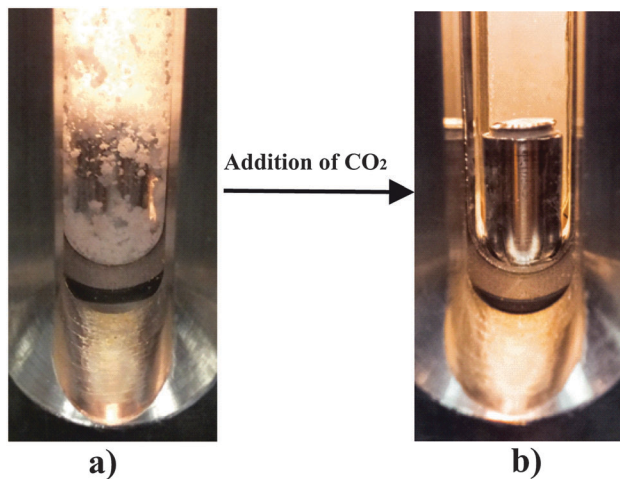


**Fig. 2** (a) Initial equimolar acetone-water mixture saturated with ibuprofen at 10 MPa and 308 K. (b) Complete dissolution of ibuprofen in the microemulsions after the isothermal and isobaric addition of CO<sub>2</sub>.

well as the Raman experiments point towards the existence of a microemulsion-like system.

In summary, in this communication we have demonstrated that surfactant-free pressurized microemulsion-like systems can be formed by adding CO<sub>2</sub> to mixtures of water and an organic solvent, such as acetone, with high mutual miscibility. The strong affinity of CO<sub>2</sub> for acetone and its low solubility in water<sup>24</sup> cause the rupture of the homogeneity of the initial water-acetone mixture and the structuration of the system at the nanoscale. Raman spectroscopy is a useful technique to characterize the microenvironment of water molecules in this system and was used to prove the existence of water-rich and water-lean nanodomains in the macroscopically transparent liquid phase. These results are promising since microemulsions with compressed CO<sub>2</sub> are an effective way to enhance the solubility of solutes. Surfactant-free CO<sub>2</sub>-based microemulsions enable more environmentally friendly process routes. Future work will include more fundamental studies of the properties of these systems and their use as templates for confined crystallizations.

This work was supported by project POMAS (Grant CTQ2010-019501) and the funding of the Erlangen Graduate School in Advanced Optical Technologies (SAOT) by the German Research Foundation (DFG) in the framework of the German excellence initiative. We also acknowledge financial support from Instituto de Salud Carlos III, through “Acciones CIBER”, with assistance from the European Regional Development Fund and the European Project BERENICE Project (305937-2). Paula Elena Rojas thanks Consejo Superior de Investigaciones Científicas (CSIC) for her PhD bursary and she is enrolled in the PhD program of UAB. Robert Hankel and Andreas Braeuer acknowledge Professors Leipertz and Will for providing access to the experimental Raman equipment.

## Notes and references

- 1 T. P. Hoar and J. H. Schulman, *Nature*, 1943, **152**, 102.
- 2 *Microemulsions: Background, New Concepts, Applications, Perspectives*, ed. C. Stubenrauch, Wiley, 2009.
- 3 D. G. Shehukin and G. B. Sukhorukov, *Adv. Mater.*, 2004, **16**, 671.
- 4 R. Wang, W. Leng, Y. Gao and L. Yu, *RSC Adv.*, 2014, **4**, 14055.
- 5 M. L. Klossek, D. Touraud, T. Zemb and W. Kunz, *ChemPhysChem*, 2012, **13**, 4116.
- 6 B. A. Keiser, D. Varie, R. E. Barden and S. L. Holt, *J. Phys. Chem.*, 1979, **83**, 1276.
- 7 B. A. Keiser and S. L. Holt, *Inorg. Chem.*, 1982, **21**, 2323.
- 8 N. F. Borys, S. L. Holt and R. E. Barden, *J. Colloid Interface Sci.*, 1979, **71**, 526.
- 9 K. P. Johnston, K. L. Harrison, M. J. Clarke, S. M. Howdle, M. P. Heitz, F. V. Bright, C. Carlier and T. W. Randolph, *Science*, 1996, **271**, 624.
- 10 C. T. Lee, W. Ryoo, P. G. Smith, J. Arellano, D. R. Mitchell, R. J. Lagow, S. E. Webber and K. P. Johnston, *J. Am. Chem. Soc.*, 2003, **125**, 3181.
- 11 J. Eastoe, C. Yan and A. Mohamed, *Curr. Opin. Colloid Interface Sci.*, 2012, **17**, 266.
- 12 M. Klostermann, T. Foster, R. Schweins, P. Lindner, O. Glatter, R. Strey and T. Sottmann, *Phys. Chem. Chem. Phys.*, 2011, **13**, 20289.
- 13 J. Zhang and B. Han, *J. Supercrit. Fluids*, 2009, **47**, 531–536.
- 14 G. D. Smith, C. E. Donelan and R. E. Barden, *J. Colloid Interface Sci.*, 1977, **60**, 488–496.
- 15 P. Traub and K. Stephan, *Chem. Eng. Sci.*, 1990, **45**, 751–758.



- 16 R. Adami, J. J. Schuster, S. Liparoti, E. Reverchon, A. Leipertz and A. Braeuer, *Fluid Phase Equilib.*, 2013, **360**, 265–273.
- 17 J. C. Elgin and J. J. Weinstock, *J. Chem. Eng. Data*, 1959, **4**, 3–12.
- 18 B. Renault, E. Cloutet, H. Cramail, T. Tassaing and M. Besnard, *J. Phys. Chem. A*, 2007, **111**, 4181–4187.
- 19 D. M. Carey and G. M. Korenowski, *J. Chem. Phys.*, 1998, **108**, 2669–2675.
- 20 G. E. Walrafen, M. S. Hokmabadi and W. H. Yang, *J. Chem. Phys.*, 1986, **85**, 6964–6969.
- 21 M. Becucci, S. Cavalieri, R. Eramo, L. Fini and M. Materazzi, *Appl. Opt.*, 1999, **38**, 928–931.
- 22 O. S. Knauer, M. C. Lang, A. Braeuer and A. Leipertz, *J. Raman Spectrosc.*, 2011, **42**, 195–200.
- 23 T. Kawamoto, S. Ochiai and H. Kagi, *J. Chem. Phys.*, 2004, **120**, 5867–5870.
- 24 P. G. Jessop and B. Subramaniam, *Chem. Rev.*, 2007, **107**, 2666–2694.
- 25 J. Manrique and F. Martinez, *Lat. Am. J. Pharm.*, 2007, **26**, 344–354.
- 26 D. Suleiman, L. A. Estévez, J. C. Pulido, J. E. García and C. Mojica, *J. Chem. Eng. Data*, 2005, **50**, 1234–1241.
- 27 M. Muntó, N. Ventosa, S. Sala and J. Veciana, *J. Supercrit. Fluids*, 2008, **47**, 147–153.

